RESEARCH PAPER

Novel synthesized attapulgite nanoparticles–based hydrophobic monolithic column for in-tube solid-phase microextraction of thiosildenafil, pseudovardenafil, and norneosildenafil in functional foods

Lubei Dong[1] · Yihui Chen[2] · Shubing Chen[2] · Chunyan Hou[3] · Shangyou Wang[1] · Rongrong Xuan[4] · Keyi Fang[2] ·
Tingting Wang[1] · Lihua Zhang[3] · Yukui Zhang[3]

Abstract

In this study, a novel method which involved in-tube solid-phase microextraction (SPME) using an attapulgite (ATP) nanoparticles–based hydrophobic monolithic column was successfully developed. It was coupled with high-performance liquid chromatography-ultraviolet detection for the determination of three phosphodiesterase-5 (PDE-5) inhibitors, including thiosildenafil, pseudovardenafil, and norneosildenafil, in functional foods. The monolithic column was prepared by one-step polymerization, using 3-trimethoxysilylpropyl methacrylate–modified ATP nanoparticles and 1-butyl-3-vinylimidazolium bromide (VBIMBr) as the functional monomers, and ethylene glycol dimethacrylate (EDMA) as the cross-linker. The obtained poly(ATP-VBIMBr-EDMA) monolith was characterized by scanning electron microscopy equipped with energy-dispersive analysis of X-ray, Fourier transform infrared spectroscopy, thermogravimetric analysis, and X-ray diffraction. The adsorption capacity, up to 2.00 μg/cm calculated by the Langmuir isotherm model, was about six times that of the poly(VBIMBr-EDMA) monolith. Crucial factors affecting the extraction efficiency, including sample solvent, elution solvent, flow rates of sampling loading and elution, sample loading volume, and elution volume, were investigated in details. Under the optimal in-tube SPME conditions, the proposed method showed good reproducibility with run-to-run, column-to-column, and batch-to-batch relative standard deviations less than 7.2%, and low limits of detection of 0.5–0.9 ng/mL in real samples. Thiosildenafil was detected in four types of functional foods with the contents of 1.30–4.78 μg/g. This newly proposed in-tube SPME method based on poly(ATP-VBIMBr-EDMA) monolith may provide a simple, efficient, and promising alternative to daily monitoring of PDE-5 inhibitors in functional foods.

Keywords Attapulgite · In-tube solid-phase microextraction · Monolith · Thiosildenafil · Pseudovardenafil · Norneosildenafil

✉ Tingting Wang
shiming-49@163.com

[1] College of Chemical Engineering, Ningbo University of Technology,
Ningbo 315016, Zhejiang, China

[2] Ningbo Academy of Inspection and Quarantine,
Ningbo 315012, Zhejiang, China

[3] Key Laboratory of Separation Science for Analytical Chemistry,
National Chromatographic Research and Analysis Center, Dalian
Institute of Chemical Physics, Chinese Academy of Sciences,
Dalian 116023, Liaoning, China

[4] The Affiliated Hospital of Medical School of Ningbo University,
Ningbo 315020, Zhejiang, China

Introduction

Phosphodiesterase type 5 (PDE-5) inhibitors including sildenafil, vardenafil, and their analogues, e.g., thiosildenafil (TD), pseudovardenafil (PD), and norneosildenafil (ND), are commonly used in erectile dysfunction treatment [1] (see Supplementary Information (ESM) Fig. S1). To date, more than 50 structural analogs of PDE-5 inhibitors have been found, and new analogues with slight structural modifications are emerging [2–4]. Because of their remarkable therapeutic effect, PDE-5 inhibitors are often found in a small dose as illegally added drugs. This may lead to repeated and excessive drug use, causing potential harms, such as hypotension, shock, and stroke, especially for those who take nitrate for a

long time, as they probably face serious incompatibility problem [5]. However, due to the diversity of the functional foods on market, the complex sample matrices pose challenges to the daily monitoring of PDE-5 inhibitors. Consequently, the development of reliable sample preparation methods for their determination in functional foods is critical.

High-performance liquid chromatography (HPLC) coupled with ultraviolet (UV) detection [6–12] and/or mass spectrometry (MS) [13, 14] is effective for the analysis of PDE-5 inhibitors. Although MS outperforms UV detection in terms of selectivity and sensitivity, the high price restricts its application in many laboratories. Currently, HPLC coupled with UV detection is widely used to determine PDE-5 inhibitors in herbal medicine [6], dietary supplements/fur seal ginseng pills [7, 9, 10], and human plasma/urine [8, 11, 12]. At the same time, a variety of sample pretreatment techniques have been developed to extract low-level PDE-5 inhibitors from complex matrix, e.g., magnetic molecularly imprinted polymers (MMIPs) [6–8], solid-phase extraction (SPE) [9], and liquid-liquid extraction (LLE) [10–12]. As an alternative technique, in-tube solid-phase microextraction (SPME) has been explored because of its high sensitivity, small sample volume, simplicity, low cost, and ease to automate.

Different from the fiber-based SPME, the stationary phase of in-tube SPME is coated [15], packed [16], or in situ polymerized [17, 18] inside capillaries or tubes. Especially, in situ polymerized organic-polymer monoliths have aroused extensive interest due to their inherent advantages, e.g., ease of preparation and modification, high porosity, and excellent pH stability. While monolith columns generally exhibit higher adsorption capacity compared with the coatings inside capillaries or tubes, further improvement is needed for trace compounds in real samples. Introducing nanoparticles is one of the effective ways to enhance adsorption capacity and reduce detection limit [17, 19]. We have confirmed this on the attapulgite (ATP) nanoparticles–modified monolith of poly(1-vinyl-3-(butyl-4-sulfonate) imidazolium-co-acrylamide-co-N,N'-methylenebis(acrylamide)) (poly(VBSIm-AM-MBA)) [17].

ATP is a low-cost natural fibrous nanoparticle with high specific surface area and porous structure and is easy to modify [20]. It contains three different types of water molecules (i.e., sorption water on the surface, zeolitic water in the micro-channel, and structural water) and bears reactive –OH groups after acidification treatment, very suitable to be introduced into hydrophilic monolithic column to improve its hydrophilicity so as to increase the adsorption capacity and separation efficiency [17, 21]. Cao et al. [22] also used ATP to improve the adsorption performance and the extraction efficiency of the hydrophilic molecularly imprinted monolithic resin composite. On the other hand, the surface of ATP could be modified with cetyltrimethyl ammonium bromide by ion exchange,

leading to good hydrophobic properties [23]. Taking the advantage of their high specific surface area, the introduction of ATP nanoparticles onto hydrophobic monolithic materials would improve the adsorption capacity towards hydrophobic compounds.

The goal of this work was to prepare a novel hydrophobic monolithic column by cross-linking 3-trimethoxysilylpropyl methacrylate (γ-MAPS)–modified ATP nanoparticles with the hydrophobic monomer 1-butyl-3-vinylimidazolium bromide (VBIMBr) and the cross-linker ethylene glycol dimethacrylate (EDMA), and investigated its feasibility and utility as an in-tube SPME sorbent for the determination of TD, PD, and ND from functional foods. Scanning electron microscopy equipped with energy-dispersive analysis of X-ray (SEM/EDAX), Fourier transform infrared (FTIR) spectroscopy, thermogravimetric analysis (TGA), and X-ray diffraction (XRD) were used to characterize the developed poly (ATP-VBIMBr-EDMA) monolithic column. The adsorption capacity was calculated using the Langmuir isotherm model. Besides, the effects of various factors (i.e., sample solvent, elution solvent, flow rates of sampling loading and elution, sample loading volume, and elution volume) on the extraction efficiency were examined. Finally, we coupled the optimized in-tube SPME with HPLC-UV for the quantitation of the three PDE-5 inhibitors in four types of functional foods.

Experimental

Chemicals and materials

EDMA, cyclohexanol, and 1,4-butanediol were purchased from J&K Scientific LTD (Shanghai, China). VBIMBr was obtained from Shanghai Chengjie Chemical Co. Ltd. (Shanghai, China). γ-MAPS (98%) was purchased from Sigma-Aldrich (St. Louis, MO, USA). The natural ATP was purchased from Jiangsu Xuyi Anhalt Nonmetallic Mining Ltd. (Jiangsu, China). The standards of TD, PD, and ND were purchased from Aladdin (Shanghai, China). HPLC-grade methanol was obtained from Tedia (Fairfield, OH, USA). Azobisisobutyronitrile and all the inorganic reagents (analytical grade) were obtained from Sinopharm Chemical Reagent Co., Ltd. (Shanghai, China). Ultra-pure water was obtained from a Milli-Q purification system (Millipore, Molsheim, France). Fused silica capillaries (250-μm i.d. × 375-μm o.d.) with polyimide coating were obtained from Yongnian Optical Fiber Factory (Hebei, China). A valve with six ports was supplied by Knauer (Berlin, Germany). The microporous membrane (13 mm, 0.22 μm) was supplied by Dikma (Beijing, China).

Instrumentation

The SEM/EDAX analysis was performed using a Hitachi S-4800 scanning electron microscope (Tokyo, Japan). FTIR spectroscopic experiment was carried out on a Thermo Nicolet iS50 FTIR spectrometer (Madison, WI, USA). TGA was conducted on a Netzsch TG 209 analyzer (Germany) at a heating rate of 10.00 K min^{-1} from 40 to 800 °C in N$_2$. XRD patterns were recorded by a Bruker AXS D8 advance diffractometer using Cu Kα radiation. A syringe pump (LSP01-1A) was obtained from Baoding Longer Precision Pump (Baoding, China).

Determination of TD, PD, and ND was performed at room temperature on the Shimadzu LC-20AT Prominence Liquid Chromatograph, which consisted of a Rheodyne 7725i six-port valve, two LC-20AT pumps, a SPD-20A UV/VIS detector, and a DGU-20A3R degasser unit. A Venusil XBP C18 column (250 × 4.6 mm i.d., 5 μm, Bonna-Agela Technologies, China) was used for the separation following in-tube SPME extraction. The mobile phase for HPLC separation was 20 mM ammonium acetate containing 0.1% acetic acid/methanol (25:75, v/v) at a flow rate of 1.0 mL/min. The injection volume was 20 μL, and the wavelength was set at 225 nm for detection.

Preparation of the attapulgite nanoparticles–based hydrophobic monolith

The fused silica capillary and the ATP nanoparticles were both modified by γ-MAPS according to the methods used in our previous reports [24, 25]. Subsequently, the poly (ATP-VBIMBr-EDMA) monolithic column was prepared as follows (Fig. 1). Specifically, 30 mg of γ-MAPS-ATP, 150 mg of VBIMBr, 120 mg of EDMA, 490 mg of cyclohexanol, 210 mg of 1,4-butanediol, and 3.0 mg of azobisisobutyronitrile were mixed to a uniform state with ultrasound, and then degassed with nitrogen for 5 min. The homogeneous reaction solution was pushed into the γ-MAPS-modified capillary equipped with a silicone rubber. The capillary was then submerged into a water bath at 75 °C for 20 h. The resultant monolithic column was rinsed with methanol to remove residues and cut to 10 cm for in-tube SPME.

The preparation of poly (VBIMBr-EDMA) monolithic column followed a similar procedure, except that no γ-MAPS-ATP was added.

In-tube solid-phase microextraction procedure

Although most of the in-tube SPME procedures were reported to perform on-line [15], off-line mode was used in this work to switch to a HPLC mobile phase with lower percentage of methanol, based on our previous work with a minor modification [26]. Prior to the extraction, with the valve at "load" position (see ESM Fig. S2), the poly (ATP-VBIMBr-EDMA) monolithic column (10 cm × 250 -μm i.d.) was conditioned with a carrier solution (20% methanol) by a syringe pump at a flow rate of 8 μL/min. The sample solution was loaded to a sample loop of 200 μL. Next, the valve was switched to the "inject" position. The sample solution was driven by the carrier solution and loaded onto the monolithic column at a flow rate of 8 μL/min. To reduce the residual sample and remove the interferences, the carrier solution was kept to pass through the monolithic column for 1 min. To elute the targets from the monolithic column, the valve was turned back to "load" position and the carrier solution was replaced by an elution solution (90% methanol-10% 25 mM ammonium acetate, pH 6.0), which was pumped through the monolithic column at a flow rate of 10 μL/min. The collected extracts were directly analyzed by HPLC-UV.

Sample preparation

The stock solutions of the three analytes (i.e., 0.425 mg/mL for TD, 0.36 mg/mL for PD, and 0.31 mg/mL for ND) were prepared separately in methanol and stored at 4 °C. The solutions were diluted to 1.4, 1.8, and 1.4 μg/mL for TD, PD, and ND, respectively, by 20% (v/v) methanol in water daily to optimize the in-tube SPME.

Four types of functional foods were randomly picked from the local supermarkets (Ningbo, China). Ginseng amino acid oral liquid, bazhen wine, *Cordyceps* mycelia oral liquid, and vitamin functional drink were manufactured in Jiangxi, Fujian, Fujian, and Hubei provinces in China, respectively. Each was weighed exactly 200 mg into a 5.0-mL volumetric flask and added 1.0 mL of methanol. The mixture was sonicated for 30 min, cooled to room temperature, diluted by purified water, and then filtered through 0.22-μm microporous membrane. For recovery determination, the blank functional foods were spiked by adding stock solutions at three levels before SPME.

Results and discussion

Preparation and characterization of the attapulgite nanoparticles–based hydrophobic monolith

In this work, a hydrophobic monolithic column was prepared with the introduction of ATP nanoparticles. VBIMBr, γ-MAPS-ATP, and EDMA were dispersed/dissolved in the mixture of cyclohexanol and 1,4-butanediol in order to synthesize the ATP nanoparticles–based hydrophobic monolith (Fig. 1). The effect of the amount of ATP nanoparticles on the column permeability (K) is evaluated (see ESM Table S1). The increase of ATP nanoparticles in the polymerization
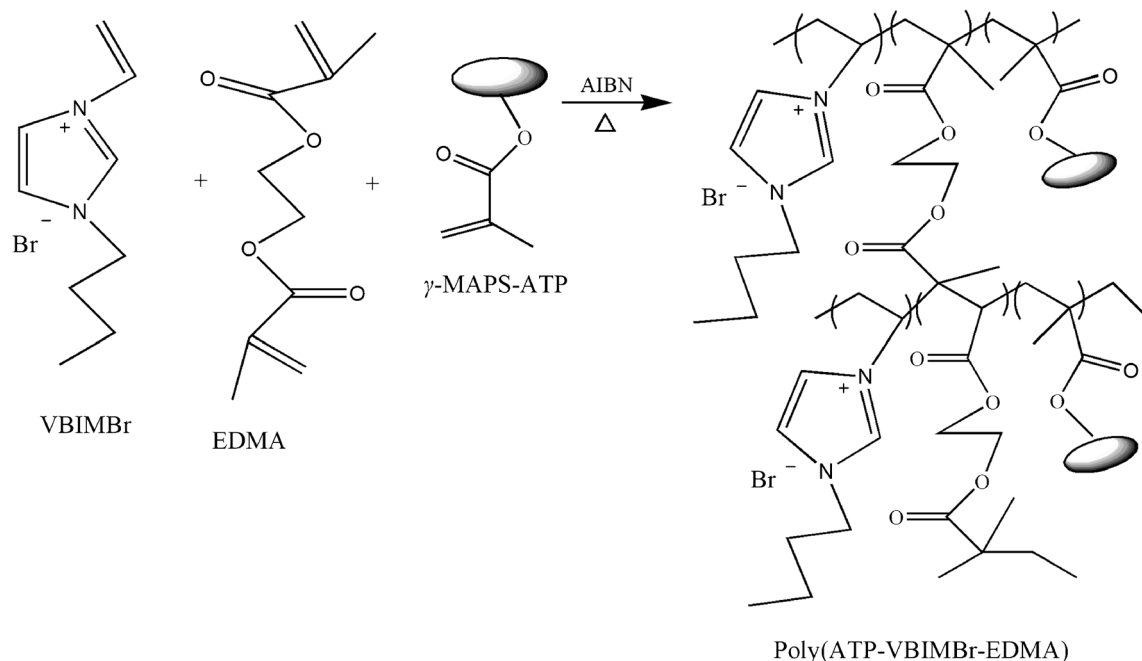
Fig. 1 Synthesis procedure of the poly (ATP-VBIMBr-EDMA) monolith

mixture resulted in a decrease in permeability, which was consistent with our reported work [17]. Aiming at higher flow rate for the in-tube SPME, the composition of column no. 2 with higher permeability was adopted in the subsequent experiments.

We also investigated the optimum flow rate range of the poly (ATP-VBIMBr-EDMA) monolithic column. A 10-cm length of the developed monolithic column was connected to an HPLC pump to monitor the permeability. As shown in Fig. S3 (see ESM), the permeability of methanol increased linearly from 0.97×10^{-14} to 4.90×10^{-14} m^2 with the flow rate increasing from 1.5 to 15 μL/min. When using water as the mobile phase, the linear range of the flow rate was from 2.5 to 12 μL/min. The sorbent would be pushed out of the capillary when the flow rate was further increased. Therefore, a flow rate less than 12 μL/min would be suitable for the in-tube SPME.

To determine the adsorption capacity, a 6-cm length monolithic column was equilibrated with 20% (v/v) methanol in water, and then loaded with 100 μL of ND at different concentrations dissolved in 20% (v/v) methanol in water. Finally, the flow-through was gathered in a centrifuge tube and determined by HPLC. The amount of ND adsorbed on the monolithic column (Q_e, μg/cm) can be calculated according to the following equation:

$$Q_e = (C_0 - C_t)V/L$$

where C_0 and C_t refer to the concentration of ND before and after passing through the monolithic column (μg/mL), respectively; V represents the sample loading volume (mL); and L denotes the length of the monolithic column (cm). For the

poly (VBIMBr-EDMA) monolithic column, the adsorbed amount of ND increases with the increase of the loading concentration and reaches a plateau (Fig. 2a). The adsorption capacity was calculated to be 0.34 μg/cm accordingly. On the contrary, the adsorption capacity of the poly (ATP-VBIMBr-EDMA) monolithic column is far from the maximum value (Fig. 2b). Therefore, the Langmuir isotherm model is used with the following equation:

$$C_t/Q_e = C_t/Q_0 + 1/K_L Q_0$$

where Q_0 refers to the maximum adsorption capacity (μg/cm) and K_L denotes the Langmuir isotherm constant (mL/μg). As shown in Fig. 2c and 2d, the linear equations of the poly (VBIMBr-EDMA) monolithic column and the poly (ATP-VBIMBr-EDMA) monolithic column are $y = 2.928x + 0.035$ and $y = 0.493x + 0.469$, respectively ($R^2 > 0.99$). Based on the slopes of the equations, the maximum adsorption capacities were calculated to be 0.34 and 2.00 μg/cm, respectively. The results demonstrated that the ATP nanoparticles significantly improved the adsorption capacity of the monolithic column. The reason for this phenomenon might be that the introduction of ATP nanoparticles could increase the number of hydrophobic groups immobilized on the monolith.

SEM images of the ATP nanoparticles–based hydrophobic monolithic column are presented in Fig. 3a and 3b. Clearly, the poly (ATP-VBIMBr-EDMA) monolith is not only uniformly continuous but also attaching closely to the inner wall of the capillary (Fig. 3a). The fiber surface is covered with a layer of polymer, and a network skeleton is formed between them (Fig. 3b). The continuous macropores together with the discrete mesopores were formed in a crisscross pattern,
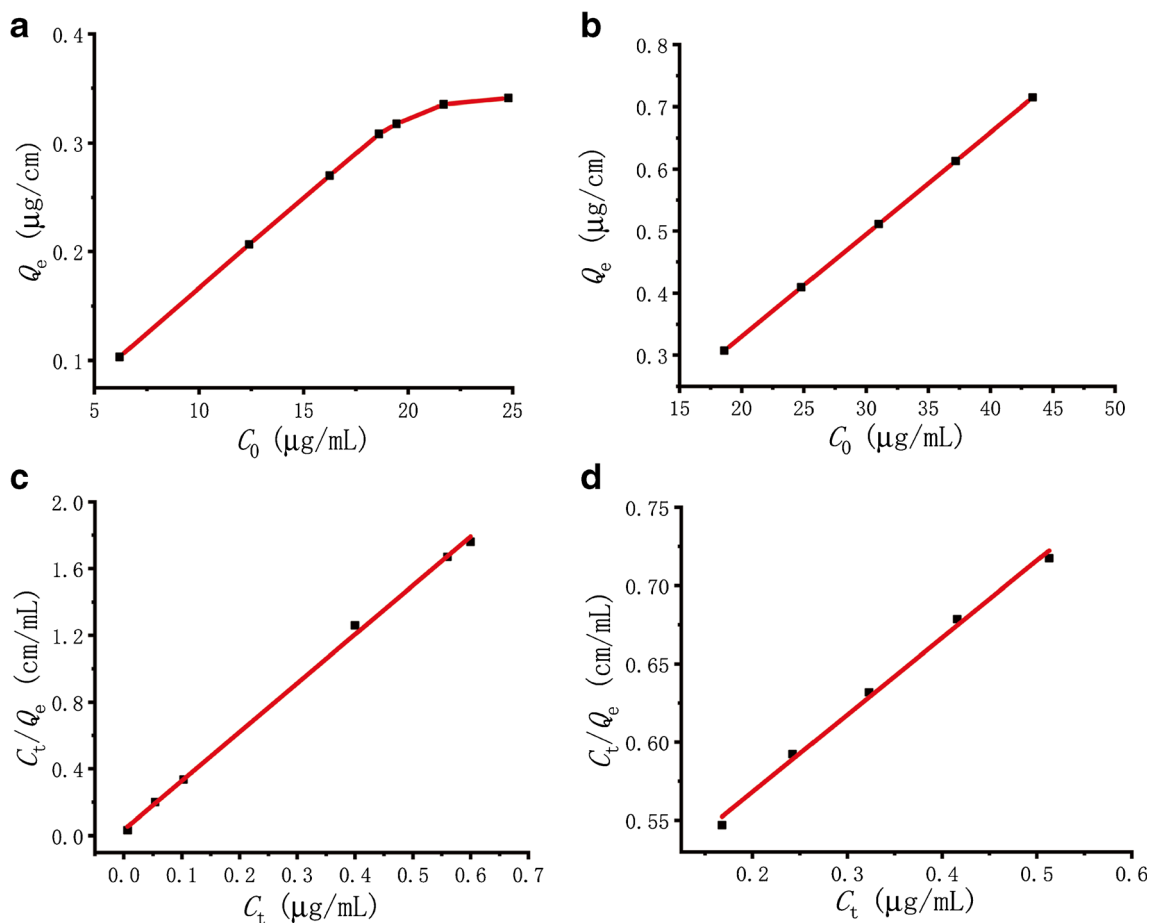
Fig. 2 Adsorption isotherms of ND on the poly (VBIMBr-EDMA) monolith (**a**) and the poly (ATP-VBIMBr-EDMA) monolith (**b**), and the related Langmuir adsorption models of ND on the poly (VBIMBr-EDMA) monolith (**c**) and the poly (ATP-VBIMBr-EDMA) monolith (**d**)

leading to low back-pressure. It was demonstrated that this monolithic structure would be suitable for in-tube SPME. EDAX spectra of acidified ATP nanoparticles and the poly (ATP-VBIMBr-EDMA) monolithic column are illustrated in Fig. 3c and 3d, respectively. The oxygen, magnesium, aluminum, silicon, and iron elements of acidified ATP nanoparticles present clear peaks (Fig. 3c). After polymerization, carbon and nitrogen elements are also confirmed in Fig. 3d. These results further demonstrated that the poly (ATP-VBIMBr-EDMA) monolith was successfully prepared.

The FTIR spectra of ATP nanoparticles, poly (VBIMBr-EDMA) monolithic column, and poly (ATP-VBIMBr-EDMA) monolithic column are compared in Fig. 4. Three peaks of ATP nanoparticles observed around 474, 800, and 985 cm^{-1} correspond to Si–O–Si stretching vibration, Al–O–Si bands, and O–H bending bands, respectively (Fig. 4a) [27, 28]. For the poly (VBIMBr-EDMA) monolithic column, the features around 1050, 1160, 1455, 1728, 2875, and 2940 cm^{-1} are attributed to the C–N stretching vibration [29], C–O–C stretching vibration [30], vibration of imidazole ring [17], C=O stretching vibration [31], –CH$_2$ stretching vibrations [32], and –CH$_3$ stretching vibrations [33], respectively (Fig.

4b). In the FTIR spectrum of the poly (ATP-VBIMBr-EDMA) monolithic column, all characteristic peaks described above are observed (Fig. 4c, ESM Table S2), indicating that the ATP nanoparticles–based hydrophobic monolithic column has been perfectly synthesized by VBIMBr, EDMA, and γ-MAPS-ATP.

The thermal property of poly (ATP-VBIMBr-EDMA) monolith is described using TGA (see ESM Fig. S4). The temperature varied from 40 to 200 °C with a weight loss of 67% which was assigned to the porogen evaporation. The loss was consistent with the content of porogen (i.e., 70%) in polymerization solution. The second weight loss (18.25%) and third weight loss (10.01%) between 200 and 440 °C represented the decomposition of the monolithic material [34]. The weight reduction range from 200 to 340 °C could be attributed to the functional groups (e.g., butyl groups, imidazole groups), while the weight loss in the other range (340–440 °C) might be due to the decomposition of the monolith backbone [35]. According to the TGA measurement, the content of organic component in the poly (ATP-VBIMBr-EDMA) monolith could be estimated as 28.26 wt%. Considering its theoretical value of 27% calculated from the feeding ratio, almost all
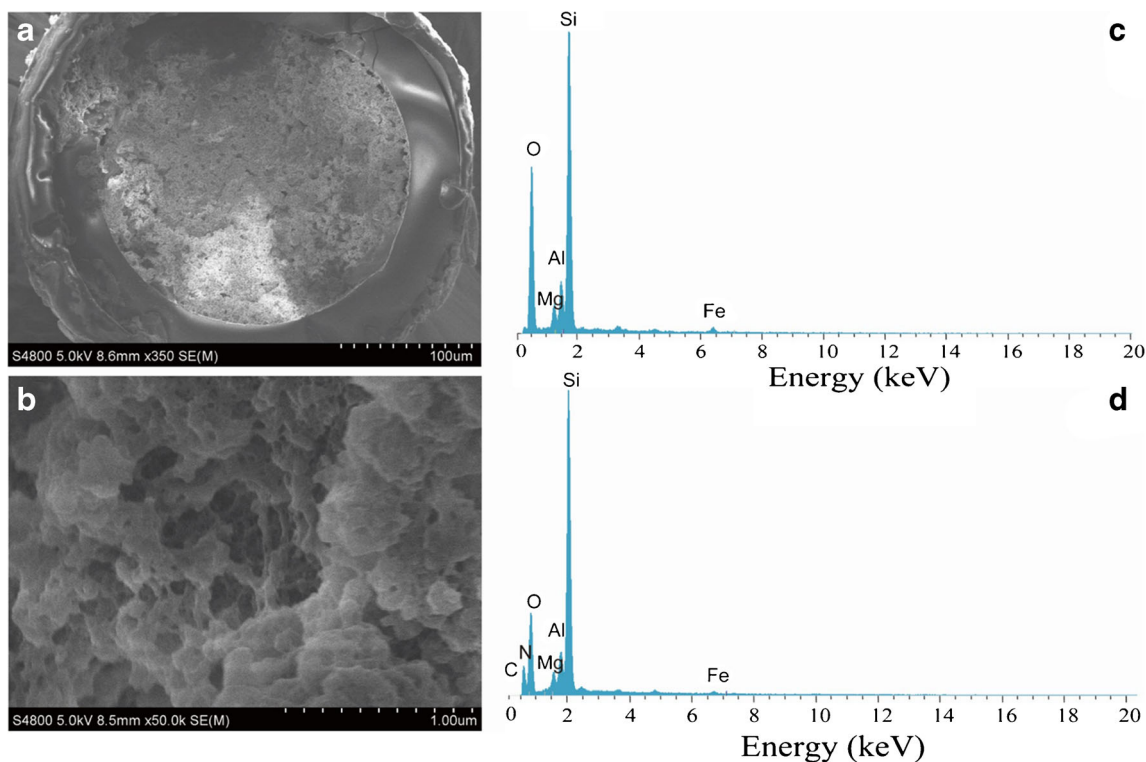
Fig. 3 SEM images of the cross section of the poly (ATP-VBIMBr-EDMA) monolith. Magnifications are 350 (**a**) and 50,000 (**b**), respectively. EDAX spectra of ATP nanoparticles (**c**) and poly (ATP-VBIMBr-EDMA) monolithic column (**d**)

VBIMBr and EDMA had been grafted onto the ATP nanoparticles.

The XRD analysis shows that the crystal structures of acidified ATP and γ-MAPS-ATP are not changed (see ESM Figs. S5A and S5B), suggesting that the modification of γ-MAPS on the surface of ATP nanoparticles will not change their crystal form. Due to the low content of ATP nanoparticles in the poly (ATP-VBIMBr-EDMA) monolithic column, only one of the strongest peaks is detected in its XRD spectrum (see ESM Fig. S5C). The XRD patterns of acidified ATP and

Fig. 4 FTIR spectra of ATP nanoparticles (**a**), poly (VBIMBr-EDMA) monolithic column (**b**), and poly (ATP-VBIMBr-EDMA) monolithic column (**c**)

γ-MAPS-ATP comfirmed the presence of SiO_2 (JCPDS: 00-005-0490) and Al_2O_3 (JCPDS: 00-050-1496) (see ESM Fig. S5). Other oxides (e.g., MgO) were not detected due to their low content.

In-tube SPME method development

In our previous works, monolithic columns were prepared by embedding ATP nanoparticles in poly(VBSIm-AM-MBA) monolith [17] or cross-linking γ-MAPS-ATP with acrylamide and N,N'-methylenebisacrylamide [21]. In this work, monolithic column for hydrophobic analytes was prepared by using a hydrophobic monomer (i.e., VBIMBr) and a cross-linking agent (i.e., EDMA). First, we investigated the effect of methanol content in the sample solution on the adsorption rate. One hundred microliters of the three targets dissolved in methanol aqueous solution at various percentages from 5 to 50% was directly loaded onto the prepared monolithic column at a flow rate of 5 μL/min, with the flow-through collected and analyzed by HPLC. The analytes were fully retained on the poly (ATP-VBIMBr-EDMA) monolithic column when the methanol contents are lower than 30% (Fig. 5a). However, the adsorption rate decreased along with the further increase of methanol percentage, in line with the typical hydrophobic mechanism. Considering the solubility of the analytes and the permeability of the prepared monolithic column, 20%
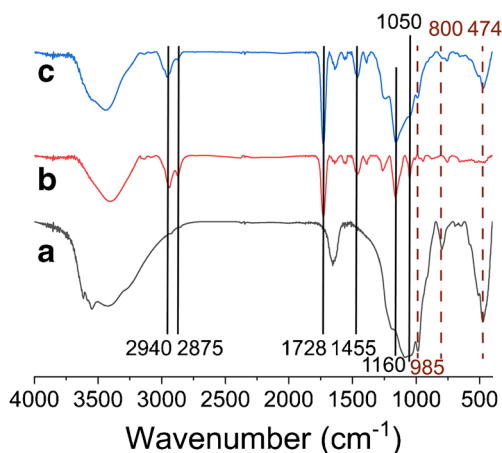
Fig. 5 Effects of the experimental conditions on the extraction efficiency of the in-tube SPME based on poly (ATP-VBIMBr-EDMA) monolithic column. Effect of the methanol content in sample solution (**a**), effect of the methanol content in elution solvent (**b**), effect of the pH value in elution solvent (**c**), effect of the ammonium acetate content in elution solvent (**d**), effect of the sample loading flow rate (**e**), effect of the elution flow rate (**f**), effect of the sample loading volume (**g**), and effect of the elution volume (**h**)
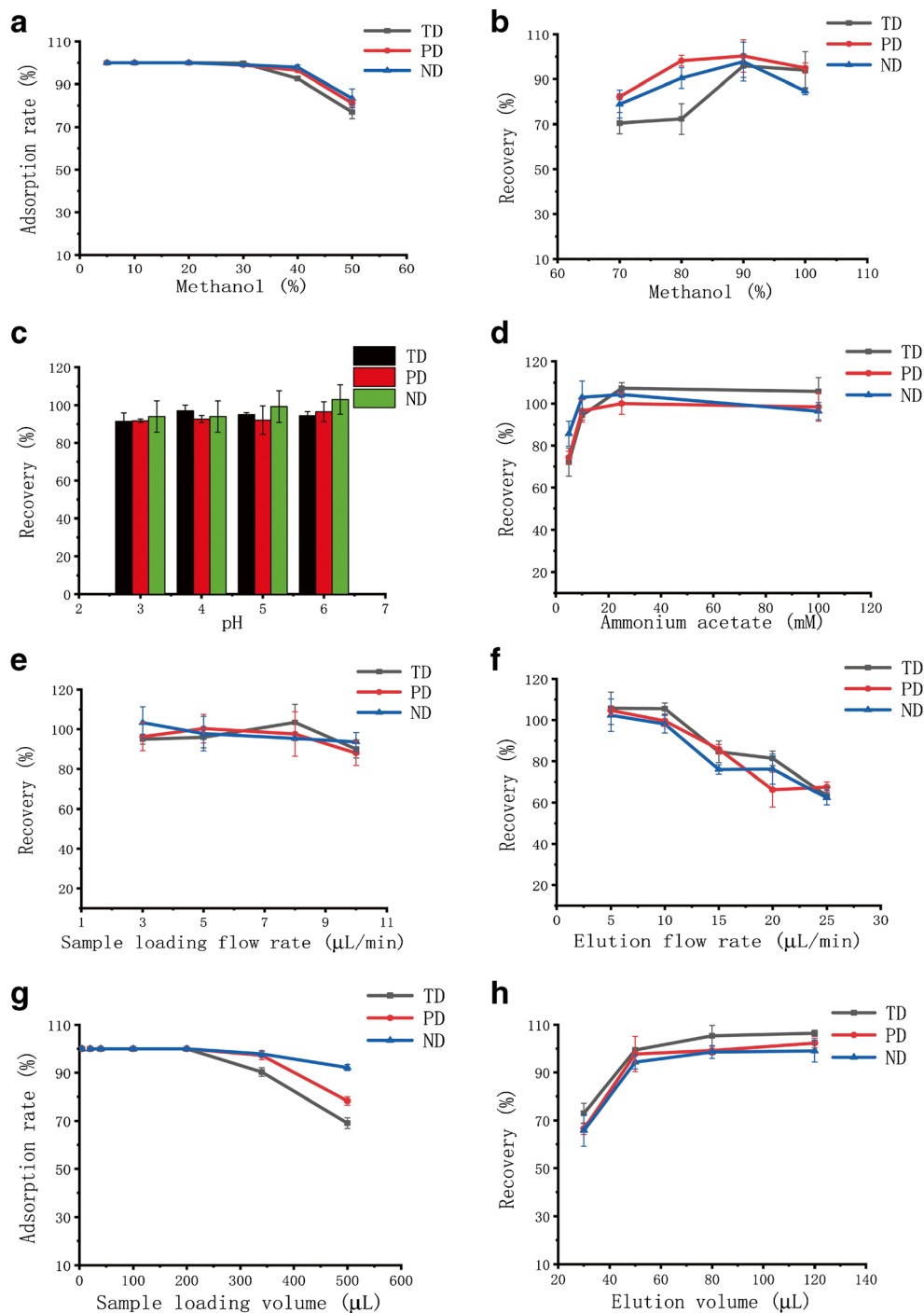
(v/v) methanol in water was chosen as the sample solution in the following study.

We further investigated the effect of methanol on the extraction efficiency via varying its content from 70 to 100% in the elution solvent. As shown in Fig. 5b, the recoveries rise to a maximum as the methanol percentage increases to 90%, and then decrease with the increase of methanol percentage. The results further verified the hydrophobic mechanism underlying the interaction between the analytes and the prepared monolithic column. However, the recoveries decreased when the methanol percentage reached 100%, due to other mechanisms such as electrostatic interactions. Hence, 90% (v/v) methanol in water was selected as the extraction solvent in subsequent experiments.

The pH value of the elution solvent affects the ionization status of weak acids or bases, thus influencing the extraction efficiency. Therefore, we explored the effect of the elution

Table 1 Linear relationships, LODs, and LOQs of the three PDE-5 inhibitors spiked in blank sample extract ($n = 3$)

PDE-5 inhibitor	Linear range (ng/mL)	Regression equation	R^2	$S_a{}^a$	LOD (ng/mL)	LOQ (ng/mL)
TD	10–3550	$Y = 237.38X + 1753$	0.9928	68	0.9	2.9
PD	10–4500	$Y = 341.57X + 8809$	0.9962	60	0.5	1.8
ND	10–3875	$Y = 263.06X + 5223$	0.9935	72	0.8	2.7

[a] Standard deviation of Y-intercept

solvent pH from 3.0 to 6.0 (90% v/v methanol in 10 mM ammonium acetate). The pK_a values of TD and PD are 10.9 and 9.11, respectively [36], while that of ND has not been reported. We assume that the pK_a of ND is about 10.05, because it is one of the analogues of sildenafil [36]. Therefore, in the pH range mentioned above, the three targets would be fully positively charged. For the monolithic column, due to the activated ATP nanoparticles, it contains silanol groups with pK_a of 2–9 [21]. In addition, we know that the pK_a values of imidazole are from 5.73 to 5.94 in 80–95.6% ethanol aqueous solutions [37]. Thus, the silanol groups would be partially deprotonated at pH 3.0–6.0, while the imidazole groups would be fully positively charged when pH less than 3.73–3.94 (pK_a-2) and partially charged when pH greater than 3.73–3.94 (pK_a-2). With the increase of pH, the negative charges of silanol groups would increase, leading to increased retention by electrostatic interaction. Similarly, the positive charges of the imidazole groups would decrease, leading to increased adsorption capacity due to the repulsive electrostatic interactions. Based on both of the interaction mechanisms, the retention would increase while the recoveries would decrease. However, we observed that the recoveries of PD and ND slightly increase when pH increases from 3.0 to 6.0 (Fig. 5c). The reason for the reduced adsorption and the increased recoveries might be the increased hydrophilicity of the ATP nanoparticles, since the hydrophilicity of the charged molecules was stronger than the neutral ones [38]. The pH value of 6.0 was selected in subsequent experiments.

Table 2 Recoveries of the three PDE-5 inhibitors spiked in blank functional foods ($n = 3$)

PDE-5 inhibitor	Spiked (μg/g)	Recovery (%)	RSD (%)
TD	7.25	97.3	5.4
	1.45	105.7	4.4
	0.50	103.2	5.1
PD	9.38	98.5	2.0
	1.88	97.9	5.3
	0.63	99.5	3.5
ND	7.25	95.7	5.2
	1.45	98.5	6.1
	0.50	100.9	2.2

In order to obtain the best recoveries, we further investigated the effect of the salt concentration in the elution solvent on the extraction efficiency. The recoveries increase when the concentration of ammonium acetate (pH 6.0) increases from 5 to 25 mM, and remain unchanged at the maximum, as presented in Fig. 5d. Higher salt concentration would reduce the electrostatic interactions between the positively charged targets and the negatively charged sorbent, leading to weaker adsorption. Therefore, 25 mM ammonium acetate (pH 6.0) in the elution solvent was adopted in subsequent experiments.

It is known that the flow rates of sampling loading and elution also affect the in-tube SPME procedure. The sample loading flow rate was optimized in the range of 3 to 10 μL/min. As can be seen in Fig. 5e, the recoveries approximately remain unchanged in the flow rate range from 3 to 8 μL/min, but show a downward trend with further increased flow rate. It demonstrated that a higher loading flow rate was adverse to the recoveries, since the three targets might not be fully extracted by the monolithic column [39]. Therefore, 8 μL/min was chosen as the loading flow rate in the following experiments.

The elution flow rate was also optimized. As shown in Fig. 5f, the increasing flow rate leads to a decrease of the recoveries, especially when it is greater than 10 μL/min. The increased flow rate might reduce the contact time between the analytes and the monolithic column, leading to decreased recoveries. We finally chose 10 μL/min as the elution flow rate to speed up the whole procedure.

Large loading volume and small elution volume are beneficial for lower limit of detection (LOD). Mixed standard solutions spiked with 0.028 μg TD, 0.036 μg PD, and 0.028 μg ND were prepared in seven volumes (i.e., 5, 20, 40, 100, 200, 340, and 500 μL). As shown in Fig. 5g, the three targets are adsorbed completely until the loading volume reaches 200 μL. As a result, 200 μL was selected as the sample loading volume used in subsequent experiments. With the elution volume increasing from 30 to 50 μL, the recoveries increase rapidly (Fig. 5h). Further increasing the elution volume did not cause obvious change of the extraction efficiency, indicating complete elution with 50-μL elution solvent. Thus, 50 μL of the elution volume was employed in the following studies.

Table 3 Run-to-run, column-to-column, and batch-to-batch precisions of the ATP nanoparticles–based monolithic column as in-tube SPME at spiked levels of 1.45, 1.88, and 1.45 µg/g for TD, PD, and ND, respectively ($n = 5$)

PDE-5 inhibitor	Run-to-run		Column-to-column		Batch-to-batch	
	Recovery (%)	RSD (%)	Recovery (%)	RSD (%)	Recovery (%)	RSD (%)
TD	100.3	1.2	103.4	3.0	98.8	7.2
PD	97.6	1.7	95.2	1.9	97.6	3.4
ND	98.4	2.3	99.9	4.4	97.8	6.8

Matrix effect

Since the disturbance from the co-extracting and co-eluting matrix components might influence the signal strength of the analytes, the matrix effect needs to be evaluated before real sample analysis. Two types of calibration curves were constructed by dissolving the three targets in pure solvent and in blank sample extract, respectively. The former regression equations for TD, PD, and ND are $Y = 227.41X + 2860$, $Y = 299.65X + 17,420$, and $Y = 253.28X + 13,947$, while the latter ones are $Y = 237.38X + 1753$, $Y = 341.57X + 8809$, and $Y = 263.06X + 5223$, respectively (Table 1). The matrix effects based on the slope ratios were calculated to be 1.04, 1.14, and 1.04 for TD, PD, and ND, respectively, indicating a minor enhancement of the functional food matrix on the target signals. The results were tolerable because the values were between 0.8 and 1.2 [40]. Nevertheless, the matrix-matched calibration curves were used for real sample analysis aiming at more reliable results.
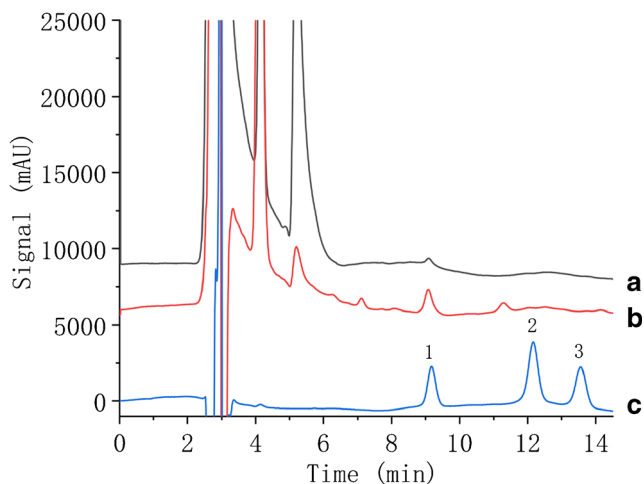

Fig. 6 Chromatograms of the three PDE-5 inhibitors: (**a**) obtained from ginseng amino acid oral liquid by direct injection mode of HPLC; (**b**) obtained from ginseng amino acid oral liquid by the proposed in-tube SPME-HPLC method; (**c**) obtained from a standard solution containing 0.71 µg/mL of TD, 0.90 µg/mL of PD, and 0.78 µg/mL of ND by direct injection mode of HPLC. Peak identification: 1, TD; 2, PD; 3, ND

Method validation

Under optimal conditions, the analytical performance of the proposed in-tube SPME was evaluated in terms of the linearities, LODs, and limits of quantification (LOQs) of the three PDE-5 inhibitors spiked in blank functional foods. As presented in Table 1, R^2 values are in the range of 0.9928–0.9962, indicating satisfactory linearities. LODs and LOQs were defined as the target concentrations at signal-to-noise ratios of 3 and 10, respectively [41]. The LODs for TD, PD, and ND were 0.9, 0.5, and 0.8 ng/mL, while the LOQs were 2.9, 1.8, and 2.7 ng/mL, respectively. Moreover, the blank functional foods were spiked at three levels of PDE-5 inhibitors before solvent extraction. Table 2 shows that the mean spiked recoveries range from 95.7 to 105.7%, with RSDs less than 6.1%, demonstrating not only the excellent accuracy but also the superior repeatability of the developed in-tube SPME based on the poly (ATP-VBIMBr-EDMA) monolithic column for the determination of PDE-5 inhibitors in functional foods.

Reproducibility

As provided in Table 3, great reproducibility and repeatable extraction performance for the run-to-run, column-to-column, and batch-to-batch ATP nanoparticles–based monolithic column as in-tube SPME are obtained, with the recoveries of the three targets in the range 95.2–103.4% and the RSDs ($n = 5$) of 1.2–7.2%.

Application to real samples

Four types of functional foods in liquid form were randomly picked from local markets and analyzed for three times under optimal in-tube SPME-HPLC conditions. The representative chromatograms are shown in Fig. 6, with an obvious enhancement of the TD peak after the in-tube SPME. As displayed in Table 4, TD is detected in the four samples in the range 1.30–4.78 µg/g with RSDs less than 4.8%, while the other two targets not detected.

The developed in-tube SPME was compared with other reported methods for the pretreatment of PDE-5 inhibitors

Table 4 Contents of the three PDE-5 inhibitors in four types of functional foods determined by the proposed method (*n* = 3)

Functional food	PDE-5 inhibitor	Content (µg/g)	RSD (%)
Ginseng amino acid oral liquid	TD	4.59	3.1
	PD	/	/
	ND	/	/
Bazhen wine	TD	1.30	4.6
	PD	/	/
	ND	/	/
Cordyceps mycelia oral liquid	TD	3.95	4.8
	PD	/	/
	ND	/	/
Vitamin functional drink	TD	4.78	1.5
	PD	/	/
	ND	/	/

"/" indicates not detected

followed by HPLC-UV/diode-array detection (DAD). As represented in Table 5, the LODs achieved using our proposed in-tube SPME method are similar to or lower than those obtained by other methods. In addition, the in-tube SPME method not only avoided large volume of toxic extraction solvent but also reduced the sample amount for one extraction by more than sixty times compared with the traditional LLE [10].

Conclusions

In this study, the poly (ATP-VBIMBr-EDMA) monolithic column was synthesized and successfully coupled with HPLC-UV for the determination of TD, PD, and ND from functional foods. The results showed that the introduction of ATP into the hydrophobic monolith increased its adsorption capacity towards hydrophobic compounds by six times. The in-tube SPME based on the poly (ATP-VBIMBr-EDMA) monolithic column exhibited high recovery, good reproducibility, and low limits of detection for function food analysis. Compared with the traditional LLE, the in-tube SPME avoided large volume of toxic extraction solvent and consumed lower sample amount for one extraction. When applied to four types of functional food samples, the proposed method produced satisfactory results, demonstrating its potential as an alternative tool for the food safety monitoring.

Table 5 Comparison of the sample preparation methods followed by HPLC-UV/DAD for the determination of PDE-5 inhibitors

Analytical method	Matrix	Number of targets	Extraction method	Sorbent	Sample amount for one extraction	LOD (ng/mL)	Recovery (%)	Ref.
HPLC-DAD	Herbal medicine samples	6	MSPE	MMIPs	60 mg	9.49–23.3	60.0–94.7	[6]
HPLC-UV	Herbal dietary supplements	3	MSPE	MMIPs	10 mg	3.66–4.15	70.91–91.75	[7]
HPLC-DAD	Human plasma human urine	2	MSPE	MMIPs	1500 µL	0.41–0.96	-	[8]
HPLC-UV	Dietary supplements	6	SPE-DLLME	Waters Oasis MCX-SPE cartridge	50 mg	2.5–7.5	76.2–114.2	[9]
HPLC-DAD	Fur seal ginseng pills	16	LLE	-	500 mg	7.0–1880	88.3–103.1	[10]
HPLC-UV	Human plasma	1	Back-extraction	-	750 µL	2	78.4–79.0	[11]
HPLC-UV	Human plasma	3	DLLME -back extraction	-	960 µL	0.92–2.69	100.4–103.9	[12]
HPLC-UV	Functional foods	3	In-tube SPME	Poly (ATP-VBIMBr-EDMA) monolith	8 mg	0.5–0.9	95.7–105.7	Current study

MSPE, magnetic solid-phase extraction; *DLLME*, dispersive liquid-liquid microextraction; "-" indicates not mentioned

Compliance with ethical standards

Conflict of interest The authors declare that they have no conflicts of interest.

References

1. Lee W, Kim HJ, Lee ME, Kim BH, Park S, Lee JH, et al. Reliable screening and classification of phosphodiesterase type 5 inhibitors in dietary supplements using gas chromatography/mass spectrometry combined with specific common ions. J Chromatogr A. 2020;162:461210.

2. Kee C, Ge X, Gilard V, Malet-Martino M, Low M. A review of synthetic phosphodiesterase type 5 inhibitors (PDE-5i) found as adulterants in dietary supplements. J Pharm Biomed Anal. 2017;147:250–77.

3. Wang Z, Wu C, Wang G, Zhang Q, Zhang J. Novel strategy for the determination of illegal adulterants in health foods and herbal medicines using high-performance liquid chromatography with high-resolution mass spectrometry. J Sep Sci. 2015;38(6):925–35.

4. Ren Y, Wu C, Zhang J. Simultaneous screening and determination of 18 illegal adulterants in herbal medicines and health foods for male sexual potency by ultra-fast liquid chromatography electrospray ionization tandem mass spectrometry. J Sep Sci. 2012;35(21):2847–57.

5. Skalicka-Wozniak K, Georgiev MI, Orhan IE. Adulteration of herbal sexual enhancers and slimmers: the wish for better sexual well-being and perfect body can be risky. Food Chem Toxicol. 2016;108(Pt B):355–64.

6. Chen FF, Xie XY, Shi YP. Magnetic molecularly imprinted polymer for the selective extraction of sildenafil, vardenafil and their analogues from herbal medicines. Talanta. 2013;115:482–9.

7. Ding M, Wu X, Yuan L, Wang S, Li Y, Wang R, et al. Synthesis of core–shell magnetic molecularly imprinted polymers and detection of sildenafil and vardenafil in herbal dietary supplements. J Hazard Mater. 2011;191(1–3):177–83.

8. Tang M, Wang Q, Jiang M, Xu L, Shi ZG, Zhang T, et al. Magnetic solid-phase extraction based on methylcellulose coated-Fe_3O_4-SiO_2-phenyl for HPLC-DAD analysis of sildenafil and its metabolite in biological samples. Talanta. 2014;130:427–32.

9. Li J, Roh SH, Shaodong J, Hong JY, Lee DK, Shin BK, et al. Solid-phase-extraction-assisted dispersive liquid-liquid microextraction based on solidification of floating organic droplet to determine sildenafil and its analogues in dietary supplements. J Sep Sci. 2017;40(15):3120–9.

10. Wang K, Zeng H, Zhang Y, Xie X, Yue Z, Zhang W, et al. A hierarchical screening method for detection of illegal adulterants in fur seal ginseng pills by profiling analysis of HPLC multi-dimensional fingerprints. J Sep Sci. 2019;42(8):1509–19.

11. Al-Hroub H, Alkhawaja B, Alkhawaja E, Arafat T. Sensitive and rapid HPLC-UV method with back-extraction step for the determination of sildenafil in human plasma. J Chromatogr B. 2016;1009–1010:1–6.

12. Xiao C, Tang M, Li J, Yin C, Xiang G, Xu L. Determination of sildenafil, vardenafil and aildenafil in human plasma by dispersive liquid-liquid microextraction-back extraction based on ionic liquid and high performance liquid chromatography-ultraviolet detection. J Chromatogr B. 2013;931:111–6.

13. Pistos C, Papoutsis I, Dona A, Stefanidou M, Athanaselis S, Maravelias C, et al. Off-line HPLC method combined to LC-MS for the determination of sildenafil and its active metabolite in post-mortem human blood according to confirmation criteria. Forensic Sci Int. 2008;178(2–3):192–8.

14. Johnson RD, Lewis RJ, Angier MK. The postmortem distribution of vardenafil (Levitra) in an aviation accident victim with an unusually high blood concentration. J Anal Toxicol. 2007;31(6):328–33.

15. Fernández-Amado M, Prieto-Blanco MC, Lopez-Mahía P, Muniategui-Lorenzo S, Prada-Rodríguez D. Strengths and weaknesses of in-tube solid-phase microextraction: a scoping review. Anal Chim Acta. 2016;906:41–57.

16. Manbohi A, Ahmadi SH. In-tube magnetic solid phase microextraction of some fluoroquinolones based on the use of sodium dodecyl sulfate coated Fe_3O_4 nanoparticles packed tube. Anal Chim Acta. 2015;885:114–21.

17. Wang TT, Chen YH, Ma JF, Qian Q, Jin ZF, Zhang LH, et al. Attapulgite nanoparticles-modified monolithic column for hydrophilic in-tube solid-phase microextraction of cyromazine and melamine. Anal Chem. 2016;88(3):1535–41.

18. Pang J, Song X, Huang X, Yuan D. Porous monolith-based magnetism-reinforced in-tube solid phase microextraction of sulfonyl-urea herbicides in water and soil samples. J Chromatogr A. 1613;2020:460672.

19. Pang J, Liao Y, Huang X, Ye Z, Yuan D. Metal-organic framework-monolith composite-based in-tube solid phase microextraction on-line coupled to high-performance liquid chromatography-fluorescence detection for the highly sensitive monitoring of fluoroquinolones in water and food samples. Talanta. 2019;199:499–506.

20. Wang T, Chen D, Lubeckyj RA, Shen X, Yang Z, McCool EN, et al. Capillary zone electrophoresis-tandem mass spectrometry for top-down proteomics using attapulgite nanoparticles functionalized separation capillaries. Talanta. 2019;202:165–70.

21. Chai MS, Chen YH, Xuan RR, Ma JF, Wang TT, Qiu D, et al. Preparation of attapulgite nanoparticles-based hybrid monolithic column with covalent bond for hydrophilic interaction liquid chromatography. Talanta. 2018;189:397–403.

22. Cao J, Wang M, Han D, Qiao F, Yan H. Attapulgite/hydrophilic molecularly imprinted monolithic resin composite for the selective recognition and sensitive determination of plant growth regulators in cucumbers. Food Chem. 2019;297:124974.

23. Xuan R, Wang T, Hou C, Li X, Li Y, Chen Y, et al. Determination of vitamin A in blood serum based on solid-phase extraction using cetyltrimethyl ammonium bromide-modified attapulgite. J Sep Sci. 2019;42(23):3521–7.

24. Wang TT, Ma JF, Zhu GJ, Shan YC, Liang Z, Zhang LH, et al. Integration of capillary isoelectric focusing with monolithic immobilized pH gradient, immobilized trypsin microreactor and capillary zone electrophoresis for on-line protein analysis. J Sep Sci. 2010;33(20):3194–200.

25. Wang T, Chen Y, Ma J, Jin Z, Chai M, Xiao X, et al. A polyethyleneimine-modified attapulgite as a novel solid support in matrix solid-phase dispersion for the extraction of cadmium traces in seafood products. Talanta. 2018;180:254–9.

26. Wang T, Chen Y, Ma J, Hu M, Li Y, Fang J, et al. A novel ionic liquid-modified organic-polymer monolith as the sorbent for in-tube solid-phase microextraction of acidic food additives. Anal Bioanal Chem. 2014;406(20):4955–63.

27. Fan QH, Shao DD, Hu J, Wu WS, Wang XK. Comparison of Ni^{2+} sorption to bare and ACT-graft attapulgites: effect of pH, temperature and foreign ions. Surf Sci. 2008;602(3):778–85.

28. Huang J, Liu Y, Jin Q, Wang X, Yang J. Adsorption studies of a water soluble dye, Reactive Red MF-3B, using sonication-surfactant-modified attapulgite clay. J Hazard Mater. 2007;143(1–2):541–8.

29. Chandran A, Varghese HT, Panicker CY, Rajendran G. FT-IR and computational study of sulphaguanidine. Orient J Chem. 2011;27(2):611–7.

30. Sen M, Erboz EN. Determination of critical gelation conditions of j-carrageenan by viscosimetric and FT-IR analyses. Food Res Int. 2010;43(5):1361–4.

31. Kumutha K, Alias Y. FTIR spectra of plasticized grafted natural rubber-$LiCF_3SO_3$ electrolytes. Spectrochim Acta A. 2006;64(2):442–7.

32. Ma C, Yang H, Zhou X, Wu B, Zhang G. Polymeric material for anti-biofouling. Colloid Surf B. 2012;100:31–5.

33. Himmelhaus M, Eisert F, Buck M, Grunze M. Self-assembly of n-alkanethiol monolayers. A study by IR-visible sum frequency spectroscopy (SFG). J Phys Chem B. 2000;104:576–84.

34. Zhang N, Qiu H, Si Y, Wang W, Gao J. Fabrication of highly porous biodegradable monoliths strengthened by graphene oxide and their adsorption of metal ions. Carbon. 2011;49(3):827–37.

35. Liu P, Jiang L, Zhu L, Wang A. Novel approach for attapulgite/poly(acrylic acid) (ATP/PAA) nanocomposite microgels as selective adsorbent for Pb(II) ion. React Funct Polym. 2014;74:72–80.

36. Singh S, Prasad B, Savaliya AA, Shah RP, Gohil VM, Kaur A. Strategies for characterizing sildenafil, vardenafil, tadalafil and their analogues in herbal dietary supplements, and detecting counterfeit products containing these drugs. Trends Anal Chem. 2009;28(1):13–28.

37. Oszczapowicz J, Czuryłowska M. The pK_a values of the conjugate acid of imidazole in water-ethanol mixtures. Talanta. 1984;31(7):559–60.

38. Greco G, Grosse S, Letzel T. Study of the retention behavior in zwitterionic hydrophilic interaction chromatography of isomeric hydroxy- and aminobenzoic acids. J Chromatogr A. 2012;1235:60–7.

39. Jiang N, Wang J, Li W, Xiao J, Li J, Lin X, et al. Silver nanoparticles-coated monolithic column for in-tube solid-phase microextraction of monounsaturated fatty acid methyl esters. J Chromatogr A. 2019;1585:19–26.

40. Frenich AG, Romero-González R, Gómez-Pérez ML, Vidal JL. Multi-mycotoxin analysis in eggs using a QuEChERS-based extraction procedure and ultra-high-pressure liquid chromatography coupled to triple quadrupole mass spectrometry. J Chromatogr A. 2011;1218(28):4349–56.

41. Shrivastava A, Gupta VB. Methods for the determination of limit of detection and limit of quantitation of the analytical methods. Chron Young Sci. 2011;2:21–5.